Protection from liver fibrosis by a peroxisome proliferator-activated receptor δ agonist

Keiko Iwaisako[a,b], Michael Haimerl[a], Yong-Han Paik[a,c], Kojiro Taura[a], Yuzo Kodama[a], Claude Sirlin[b], Elizabeth Yu[d], Ruth T. Yu[d], Michael Downes[d], Ronald M. Evans[d,1], David A. Brenner[a], and Bernd Schnabl[a,1]

Departments of [a]Medicine and [b]Radiology, University of California at San Diego, La Jolla, CA 92093; [c]Department of Internal Medicine, Samsung Medical Center, Sungkyunkwan University School of Medicine, Seoul 135-710, Korea; and [d]Gene Expression Laboratory, Salk Institute for Biological Studies, La Jolla, CA 92037

Contributed by Ronald M. Evans, March 28, 2012 (sent for review November 18, 2011)

Peroxisome proliferator-activated receptor delta (PPARδ), a member of the nuclear receptor family, is emerging as a key metabolic regulator with pleiotropic actions on various tissues including fat, skeletal muscle, and liver. Here we show that the PPARδ agonist KD3010, but not the well-validated GW501516, dramatically ameliorates liver injury induced by carbon tetrachloride (CCl_4) injections. Deposition of extracellular matrix proteins was lower in the KD3010-treated group than in the vehicle- or GW501516-treated group. Interestingly, profibrogenic connective tissue growth factor was induced significantly by GW501516, but not by KD3010, following CCl_4 treatment. The hepatoprotective and antifibrotic effect of KD3010 was confirmed in a model of cholestasis-induced liver injury and fibrosis using bile duct ligation for 3 wk. Primary hepatocytes treated with KD3010 but not GW501516 were protected from starvation or CCl_4-induced cell death, in part because of reduced reactive oxygen species production. In conclusion, our data demonstrate that an orally active PPARδ agonist has hepatoprotective and antifibrotic effects in animal models of liver fibrosis, suggesting a possible mechanistic and therapeutic approach in treating patients with chronic liver diseases.

hepatic stellate cells | Kupffer cells | liver cirrhosis

Liver fibrosis is a common consequence of chronic liver injury including alcohol abuse, viral hepatitis, autoimmune disease, and nonalcoholic steatohepatitis. Chronic liver disease can progress to cirrhosis and hepatocellular carcinoma. Cirrhosis is a major health burden worldwide and currently is the 12th leading cause of death in the United States. Liver fibrosis is reversible if the causative agent (e.g., alcohol consumption, hepatitis B and C viral infections, or biliary obstruction) is removed successfully (1). However, the underlying causative agent is treated successfully only in subsets of patients with liver diseases, and there are no specific treatments for liver fibrosis. An ideal antifibrotic therapy would be liver specific, well tolerated when administered for prolonged periods of time, and effective in attenuating excessive collagen deposition without affecting normal extracellular matrix synthesis (2).

Peroxisome proliferator-activated receptors (PPARs) are members of the nuclear receptor family of ligand-activated transcription factors. They form heterodimers with retinoid X receptor (RXR) and bind to consensus DNA sites. Ligand binding induces a conformational change in PPAR–RXR complexes, releasing repressors in exchange for coactivators, and results in modulation of gene transcription. PPARs are able to transrepress as well as transactivate genes (3). Functional dissection of ligand-dependent coregulators of PPARs reveals that their transcriptional regulation is linked to histone modification and chromatin remodeling. All three subtypes of PPARs, including PPARδ, can be activated by fatty acids and fatty-acid derivatives. Based on studies using gene deletion and synthetic agonists, PPARδ is emerging as a key metabolic regulator. PPARδ agonists improve glucose and lipid homeostasis (4, 5) and increase skeletal muscle fatty-acid metabolism. PPARδ agonists have been shown to be exercise mimetics and to increase endurance in mice that already are undergoing exercise (6). PPARδ has anti-inflammatory activities, including inhibition of cytokine production and promoting the alternative activation of macrophages (7).

To determine whether PPARδ agonists are beneficial in experimental liver fibrosis, mice were treated orally with a PPARδ agonist, KD3010, or with the well-validated PPARδ agonist GW501516. Unexpectedly, KD3010, but not GW501516, showed hepatoprotective and antifibrotic effects in liver fibrosis induced by carbon tetrachloride (CCl_4) or bile duct ligation (BDL).

Results

PPARδ Agonist KD3010 Protects from Liver Injury. Liver injury was induced by repeated injections of CCl_4, and mice were treated daily with vehicle, the widely used PPARδ agonist GW501516 (6), or the PPARδ agonist KD3010 by oral gavage. Control oil-injected mice did not show any liver damage (Fig. 1*A*). Liver injury consisting of hepatocyte death and inflammation was seen in the vehicle- or GW501516-treated group injected with CCl_4 on H&E-stained liver sections but was markedly reduced in the KD3010-treated group (Fig. 1*A*). This result was confirmed by serum alanine aminotransferase (ALT) levels, which were reduced only in the KD3010 group compared with other groups (Fig. 1*B*). Both KD3010 and GW501516 induced PPARδ-responsive genes such as adipose differentiation-related protein (*ADFP*) and uncoupling protein 2 (*UCP2*), but not PPARα- and PPARγ-specific responsive genes such as *FGF21* and *CD36,* respectively (Fig. 1*C*).

KD3010-Treated Mice Show Less Hepatic Fibrosis. Fibrillar collagen deposition as a measure of liver fibrosis was determined by Sirius Red staining. Vehicle- or GW501516-treated animals showed bridging fibrosis. Fibrosis was lower in the KD3010 group (Fig. 1*D*) than in the other groups. The lower level of Sirius Red staining was confirmed by morphometric analysis (Fig. 1*E*). Hydroxyproline content, a measure for total collagen, was reduced in the KD3010 group (Fig. 1*F*). Mice subjected to CCl_4 and treated with KD3010 showed control levels of the inflammatory cytokine *TNFα* compared with the vehicle- and GW501516-treated groups (Fig. 1*G*). Similarly, α-smooth muscle actin (*αSMA*) mRNA, a marker of hepatic stellate cell activation, also was down-regulated in the KD3010 group. An

Author contributions: K.I., C.S., R.T.Y., M.D., R.M.E., D.A.B., and B.S. designed research; K.I., M.H., Y.-H.P., K.T., Y.K., and E.Y. performed research; K.I., C.S., R.T.Y., M.D., R.M.E., D.A.B., and B.S. analyzed data; and K.I., D.A.B., and B.S. wrote the paper.

The authors declare no conflict of interest.

Data deposition: The microarray data reported in this paper have been deposited in the Gene Expression Omnibus (GEO) database (accession code GSE32121).

[1]To whom correspondence may be addressed. E-mail: evans@salk.edu or beschnabl@ucsd.edu.

This article contains supporting information online at www.pnas.org/lookup/suppl/doi:10.1073/pnas.1202464109/-/DCSupplemental.

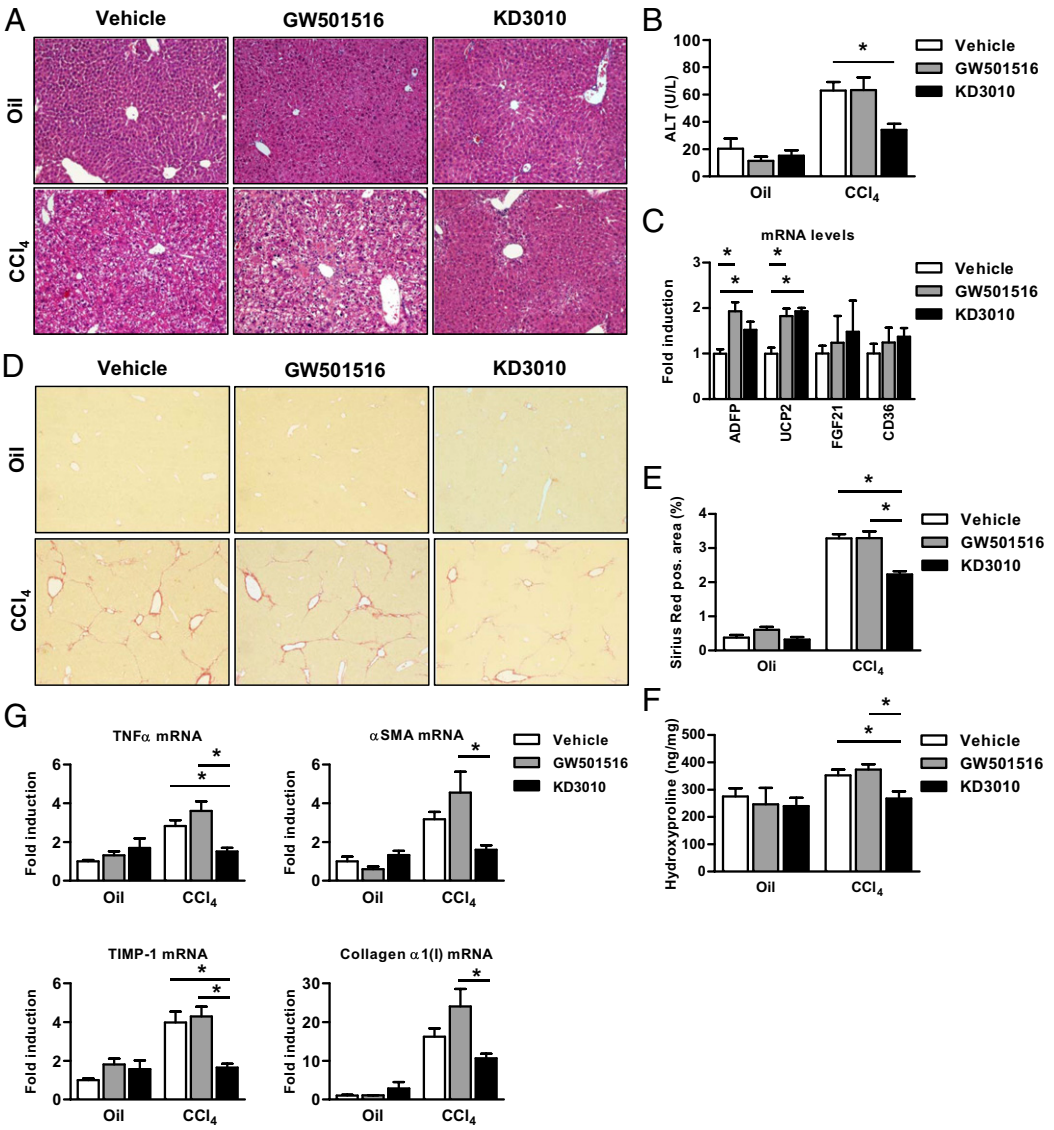

Fig. 1. Reduced liver injury and hepatic fibrosis in mice treated with the PPARδ agonist KD3010. Mice were injected i.p. 12 times with oil as control ($n = 4$ in each group) or with CCl_4 and were administered vehicle ($n = 14$), GW501516 (2 mg/kg; $n = 12$), or KD3010 (10 mg/kg; $n = 11$) daily by oral gavage. (*A*) Representative H&E-stained liver sections are shown. (*B*) ALT levels were measured in the serum of mice. (*C*) Relative gene-expression levels of *ADFP*, *UCP2*, *FGF21*, and *CD36* were determined in the liver of mice treated with vehicle, GW501516, or KD3010 for 5 wk ($n = 4$ in each group). (*D* and *E*) Collagen deposition was evaluated by Sirius Red staining and quantitated by image analysis. Representative sections stained with Sirius Red are shown for vehicle-, GW501516-, and KD3010-treated mice. (*F*) Hydroxyproline content was measured in the liver of mice. (*G*) Hepatic *TNFα*, *αSMA*, *TIMP-1*, or *collagen α1(I)* gene expression was assessed by qPCR. $^*P < 0.05$.

equally impressive reduction of hepatic expression of mRNA encoding *collagen α1(I)* was found in the KD3010 group, and induction of tissue inhibitor of matrix metalloproteinases (*TIMP*)-*1*, an important mediator of liver fibrosis, was decreased in the KD3010 group (Fig. 1*G*). Taken together, PPARδ ligand activation by KD3010, but not by GW501516, protects against chemically induced liver injury and fibrosis and reduces hepatic inflammation.

KD3010 Protects Against Cholestasis-Induced Liver Fibrosis. To determine whether the PPARδ agonist KD3010 suppresses hepatic fibrosis induced by a different etiology, mice underwent cholestatic liver injury by BDL and were treated daily with vehicle or KD3010. Twenty-one days after BDL, liver injury was reduced markedly in the KD3010 group as seen on H&E-stained liver sections (Fig. 2*A*). Mice treated with KD3010 showed a significant reduction in fibrosis as evidenced by Sirius Red staining (Fig. 2 *B* and *C*). The survival rate was significantly higher in PPARδ agonist-treated mice subjected to BDL (Fig. 2*D*). In addition, compared with mice treated with vehicle, the KD3010 BDL group showed decreased expression of inflammatory genes in the liver, including *TNFα* and *IL-1β* (Fig. 2*E*). Consistent with the histopathology, hepatic *TIMP-1* and collagen α1(I) gene expression was decreased following PPARδ ligand activation (Fig. 2*E*). Thus, PPARδ activation protects from both hepatotoxic and cholestatic liver fibrosis.

Cellular Expression of PPARδ in the Liver. To determine which hepatic cells express PPARδ in vivo, we performed double staining for PPARδ and F4/80, as a marker for Kupffer cells, or desmin, as a marker for hepatic stellate cells. PPARδ protein expression was found in the nucleus of Kupffer cells and hepatic stellate cells (Fig. 3*A*). Notably, not all Kupffer cells or hepatic stellate cells expressed PPARδ, consistent with reports of heterogeneous

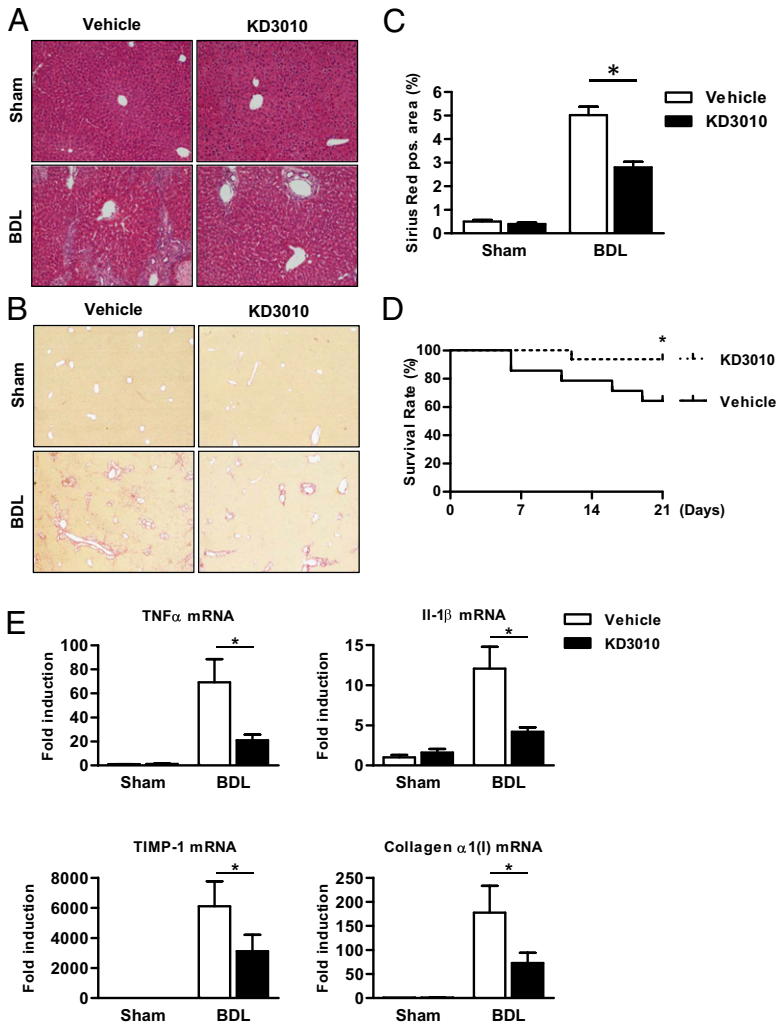

Fig. 2. Mice receiving KD3010 are protected from liver fibrosis after BDL. Mice underwent sham operation (n = 4 in each group) or BDL for 21 d and were treated with vehicle (n = 9) or KD3010 (n = 14). (*A*) Representative H&E-stained liver sections are shown. (*B* and *C*) Hepatic fibrosis was assessed by Sirius Red staining. Representative sections are shown. (*D*) Survival of mice receiving vehicle (n = 14) or KD3010 (n = 16) following BDL for 21 d. (*E*) Hepatic *TNFα*, *IL-1β*, *TIMP-1*, or *collagen α1(I)* gene expression was assessed by qPCR. *$P < 0.05$.

Kupffer cell and hepatic stellate cell populations (8). Hepatocytes showed weak positive staining for PPARδ protein. Adipose tissue was used as a positive staining control (Fig. S1).

A similar expression pattern was observed on the gene level. *PPARδ* mRNA was expressed predominantly in Kupffer cells and in hepatic stellate cells isolated from normal liver but was expressed only minimally in hepatocytes (Fig. 3*B*). To confirm the responsiveness of hepatocytes to a PPARδ ligand, hepatocytes were isolated, and expression of PPARδ-responsive genes was determined following treatment with KD3010. KD3010 induced PPARδ-responsive genes such as *ADFP*, pyruvate dehydrogenase kinase, isoenzyme 4 (*PDK4*), and angiopoietin-like 4 (*Angptl4*) but not the PPARα- and PPARγ-responsive genes, *FGF21* and *CD36*, respectively (Fig. 3*C*). These results indicate that KD3010 is capable of activating PPARδ in hepatocytes.

Polarization State of Kupffer Cells Is Not Affected by KD3010. In response to different stimuli, Kupffer cells are capable of differentiating into two polarization states, M1 and M2. LPS promotes Kupffer cell differentiation to a classical, M1 phenotype. The M1 activation pattern is responsible for up-regulating proinflammatory mediators (9). To delineate the effects of KD3010 on Kupffer cells, primary Kupffer cells were isolated from wild-type mice and cultured in the presence of KD3010. The morphology did not change following treatment with KD3010 for 1 d in culture compared with vehicle-treated cells (Fig. S2*A*). KD3010 induced PPARδ-responsive genes such as *ADFP*, *PDK4*, and *Angptl4* in primary Kupffer cells (Fig. 3*D*). LPS-induced expression of *TNFα*, *IL-6*, and *IL-1β* was not suppressed by KD3010 in cultured Kupffer cells (Fig. S2*B*). In contrast, an alternative or M2 phenotype of Kupffer cells is induced in response to IL-4 and IL-13. The M2 phenotype is thought to produce anti-inflammatory factors and to promote tissue repair after inflammation and/or injury (7, 10). IL-4–induced expression of M2 markers such as *arginase1* and macrophage galactose-type C-type lectin 1 (*Mgl-1*) was not affected following KD3010 treatment in cultured Kupffer cells (Fig. S2*B*). Thus, KD3010 induces a common set of PPARδ target genes such as *ADFP*, *PDK4*, and *Angptl4* in both M1 and M2 Kupffer cells.

PPARδ Ligand KD3010 Does Not Decrease the Activation and Fibrogenic Potential of Hepatic Stellate Cells. To explain the beneficial effect of KD3010 in liver fibrosis, we next focused on hepatic stellate cells. Hepatic stellate cells isolated from wild-type mice did not change their morphology following treatment with

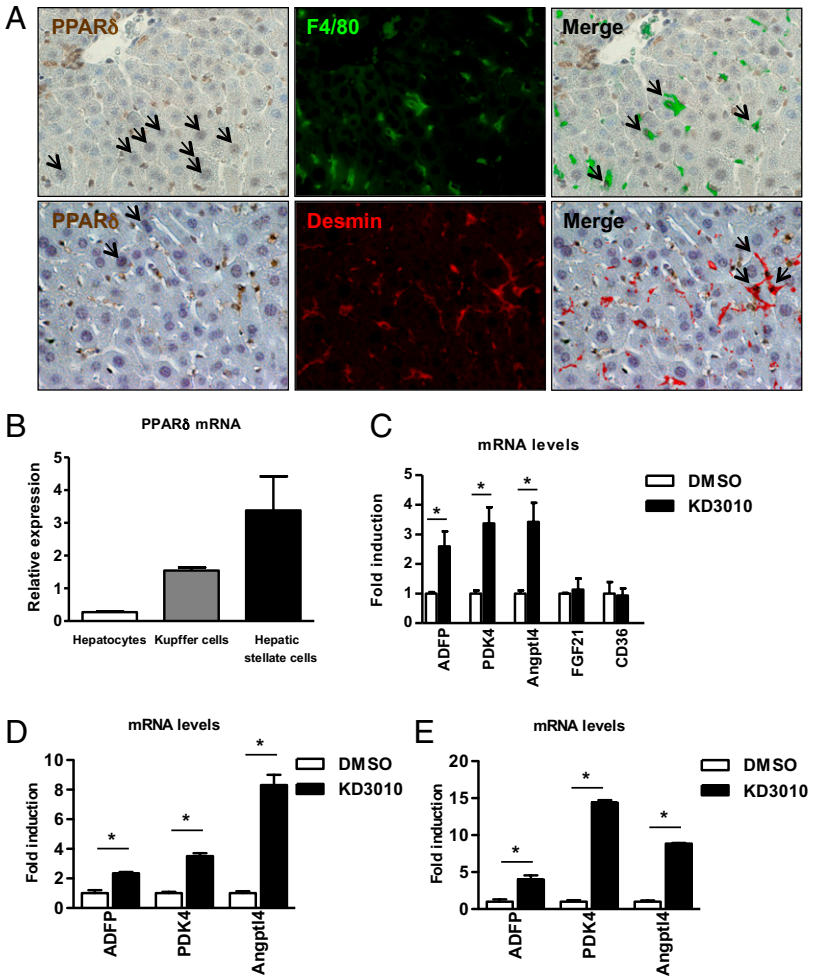

Fig. 3. Hepatocytes express PPARδ. (*A*) Immunohistochemical staining for PPARδ (brown), and immunofluorescent staining for F4/80 (green) and desmin (red) was performed to detect PPARδ protein in Kupffer cells and hepatic stellate cells, respectively. Black arrows indicate positively stained hepatocytes (*Left*), double-positive Kupffer cells (*Upper Right*), and hepatic stellate cells (*Lower Right*). (*B*) Liver cell fractions were isolated from a normal liver. PPARδ mRNA was analyzed by qPCR and normalized to 18S. The mean of three independent isolations is shown. (*C*) Hepatocytes were cultured with DMSO or KD3010 (5 μM). Gene expression of *ADFP*, pyruvate dehydrogenase kinase, isoenzyme 4 (*PDK4*), angiopoietin-like 4 (*Angptl4*), fibroblast growth factor (*FGF*)-*21*, and *CD36* was analyzed by qPCR and normalized to 18S. The mean of four independent experiments are shown. (*D*) Kupffer cells were cultured with DMSO or KD3010 (1 μM). Gene expression of *ADFP*, *PDK4*, and *Angptl4* was analyzed by qPCR and normalized to 18S. (*E*) Hepatic stellate cells were cultured with DMSO or KD3010 (1 μM). Gene expression of *ADFP*, *PDK4*, and *Angptl4* was analyzed by qPCR and normalized to 18S. $*P < 0.05$.

KD3010 for 3 d in culture compared with vehicle-treated cells (Fig. S3*A*). Although KD3010 induced PPARδ-responsive genes such as *ADFP*, *PDK4*, and *Angptl4* (Fig. 3*E*), hepatic stellate cells incubated with KD3010 showed no change in the expression of fibrogenic genes *αSMA*, *TIMP-1*, and *collagen α1*(*I*) or the proliferation marker *cyclin D1* (Fig. S3*B*). *Hepatocyte growth factor* (*HGF*) was induced in KD3010-treated hepatic stellate cells compared with control cells (Fig. S3*B*). Thus, KD3010 does not modulate fibrogenic properties of hepatic stellate cells.

PPARδ Ligand Activation Protects Hepatocytes from Starvation and CCl_4-Induced Cell Death. We then focused on hepatocytes as potential targets for the beneficial effect of KD3010 in liver injury and fibrosis. KD3010 protected cultured hepatocytes from starvation-induced cytotoxicity, as evidenced by reduced ALT in the supernatant and reduced cell death (released LDH) (Fig. 4 *A*–*C*). In addition, KD3010 protected cultured hepatocytes from CCl_4-induced cell death, as assessed by diminished propidium iodide (PI) staining (Fig. 4*D*), and reduced ALT levels in the supernatant (Fig. 4*E*). The hepatoprotective effect of KD3010 was absent in PPARδ-deficient hepatocytes (Fig. 4*E*), demonstrating that the hepatoprotection of KD3010 is not an off-target effect.

Because reduced oxidative stress might mediate the protection from cell death, reactive oxygen species (ROS) were measured and indeed were lower in CCl_4-treated hepatocytes incubated with KD3010, whereas hepatocytes incubated with GW501516 showed more ROS production (Fig. 4*F*). KD3010 treatment of wild-type hepatocytes decreased thiobarbituric acid-reactive substances (TBARS), a measure of lipid peroxidation, after CCl_4 exposure, but this effect was not seen in PPARδ-deficient hepatocytes (Fig. 4*G*). We next examined cytochrome P450 (Cyp) expression, because its function is to catalyze the oxidation of organic substances. Gene expression of several Cyp family members was induced following incubation with KD3010. However, *Cyp2E1*, the CCl_4-metabolizing enzyme, was not affected by KD3010 (Fig. 4*H*). Thus, KD3010 induces Cyp family members, decreases ROS in hepatocytes, and protects hepatocytes from starvation and toxic cell death.

To explain further the differences between KD3010 and GW501516, we compared the gene-activation profile of the two compounds in cultured hepatocytes by gene-expression micro-

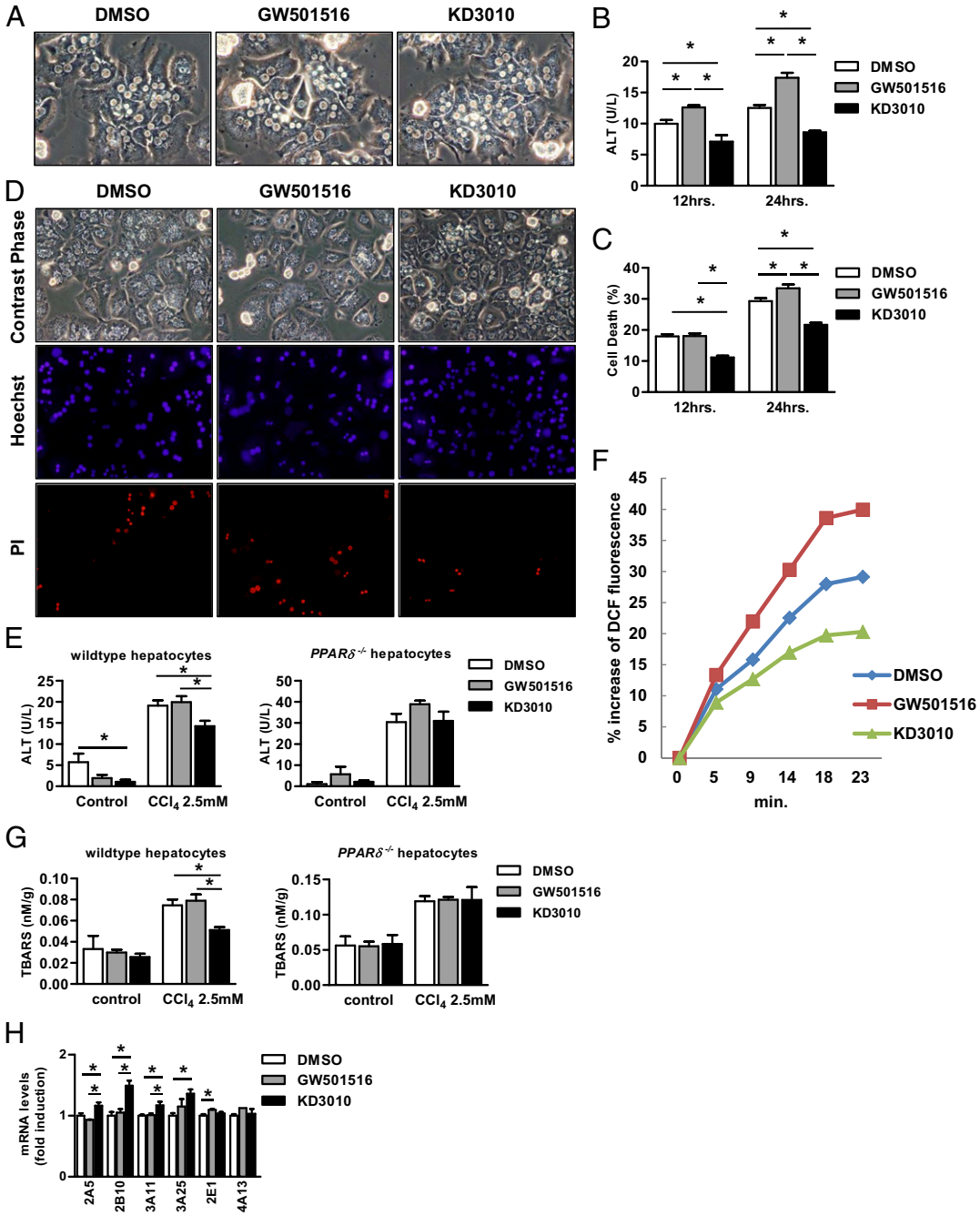

Fig. 4. KD3010 protects hepatocytes from cell death in culture. Hepatocytes were cultured in KRB without glucose and without FCS for indicated time periods in the presence of DMSO, GW501516 (100 nM), or KD3010 (5 μM). (*A*) Representative photomicrographs are shown. ALT was measured in the supernatant of cells (*B*), and cell death was assessed (*C*). (*D*) CCl_4 (2.5 mM) was added to hepatocytes after 12 h in the presence of DMSO, GW501516 (100nM) or KD3010 (5 μM). Representative photomicrographs of cells and Hoechst- and PI-stained hepatocytes are shown. (*E*) CCl_4-induced cell death was assessed in wild-type and PPARδ-deficient hepatocytes by measuring ALT in the supernatant. (*F*) Hepatocytes cultured with DMSO, GW501516 (100 nM), or KD3010 (5 μM) for 12 h were loaded with redox-sensitive dye CM-H_2DCFDA (10 μM) for 20 min. Fluorescent signals were quantified continuously for 23 min using a fluorometer. (*G*) TBARS were assessed in wild-type and PPARδ-deficient hepatocytes. (*H*) Hepatocytes were cultured in KRB in the presence of DMSO, GW501516 (100 nM) or KD3010 (5 μM) for 12 h. qRT-PCR was performed for Cyp family members. Results shown are the mean of four different hepatocyte isolations.*$P < 0.05$.

array analysis. Surprisingly, the two PPARδ agonists had distinct gene-expression profiles (Fig. S4 *A–C* and Tables S1 and S2). Known PPARδ-responsive genes such as *PDK4* and carnitine palmitoyltransferase 2 were induced by both agonists. KD3010 caused a larger change in gene expression than did GW501516. Interestingly, connective tissue growth factor (*CTGF*) was induced by GW501516 but not by KD3010. We therefore compared hepatic *CTGF* gene expression following CCl_4 treatment in mice gavaged with GW501516 or KD3010. Similar to the in vitro results, *CTGF* mRNA was significantly higher in GW501516-treated than in vehicle-treated mice, but there was no difference between KD3010- and vehicle-treated mice following repeated CCl_4 injections (Fig. S4*D*). CTGF has potent profibrogenic properties and is produced and secreted by hepatocytes (11). Recently CTGF has been shown to be induced by p53 in hepatocytes and to result in liver fibrosis (12), possibly

thereby contributing to the different effects on liver fibrosis observed with GW501516 and KD3010.

Discussion

To address the effect of PPARδ activation on chronic liver diseases, we took an unbiased approach to test a potent and highly selective PPARδ agonist, KD3010, in mouse models of liver fibrosis induced by hepatotoxicity (CCl_4 injections) and cholestasis (BDL). KD3010 shows dramatic antifibrotic effects in vivo and was more effective than the well-validated PPARδ agonist GW501516. Hepatocytes appear to be the target for PPARδ ligand activation, because KD3010 protects cultured hepatocytes from starvation- and CCl_4-induced cell death. Thus, a hepatoprotective effect upon ligand activation mediates the beneficial effect of KD3010 in experimental animal models of liver fibrosis.

The role of PPRAδ in chronic liver disease has not been examined previously. PPARδ deficiency increases acute liver toxicity induced by azoxymethane or CCl_4 in mice (13), whereas treatment with the PPARδ ligand GW0742 ameliorates acute CCl_4-induced liver toxicity in a PPARδ-dependent fashion (14). The cellular mechanism was not identified in these studies (13). In contrast to the beneficial effect of PPARδ ligand activation in acute liver disease, enhanced acute liver toxicity after one dose of CCl_4 was reported to occur in rats when another PPARδ ligand, L165041, was administered concomitantly (15). Our study demonstrates that a highly specific PPARδ agonist, KD3010, showed potent beneficial effects in two models of liver injury and fibrosis, whereas the known PPARδ agonist GW501516 did not affect chronic liver injury. Consistent with our results, GW501516 did not affect liver fibrosis in a choline-deficient, ethionine-supplemented mouse model of steatohepatitis (16). Differences in the physiological outcomes of specifically targeted nuclear receptor pharmacophores are well documented in the steroid receptor family for estrogens, glucocorticoids, and androgens. In addition, differential outcomes have been reported recently for targeted synthetic farnesoid X receptor ligands, as demonstrated by global gene-expression profiles (17). The differences reported here for the PPARδ agonists can be attributed to a number of different factors, including different specificities for other PPAR isoforms, potencies of different synthetic compounds, and in vivo pharmacological properties of the compounds including differential tissue distribution, degradation, and clearance. This study demonstrates that distinct structural pharmacophores, although classified as agonists, can confer widely differing benefits in the pathological setting when studying the effects of nuclear receptor-targeted agonists.

PPARδ plays an important role in energy, glucose, and lipid homeostasis. This role may be mediated in part by alternative M2 activation of macrophages/Kupffer cells. Genetic ablation of PPARδ in bone marrow cells impairs alternative activation of tissue macrophages and predisposes mice to the development of insulin resistance and metabolic syndrome, including adiposity and hepatic steatosis on a high-fat diet (7). PPARδ is induced by T-helper type 2 cytokines derived from hepatocytes or adipocytes to induce alternative activation of adipose tissue macrophages or Kupffer cells, suggesting that M2 macrophages have a profound influence on oxidative metabolism and lipid homeostasis. Alternatively activated macrophages attenuate inflammation in the liver and also in white fat tissue (7, 10). In contrast, recent studies do not support a role for alternative activation of macrophages mediated by PPARδ. Loss of PPARδ in bone marrow-derived cells did not affect glucose tolerance in mice fed a high-fat diet (18). PPARγ, but not PPARδ, activation promotes human monocyte differentiation toward alternative macrophages (19). Although Kupffer cells express endogenous PPARδ, our study provides evidence that Kupffer cells are not an important target for PPARδ ligand activation to mediate its antifibrotic effect. KD3010 did not modulate in vitro activation and the polarization state of Kupffer cells. Hepatic stellate cells, the main cell type producing extracellular matrix in liver fibrosis, express endogenous PPARδ, but their fibrogenic properties are not changed following PPARδ activation in vitro.

Hepatocytes, the predominant liver cell type, express PPARδ and induce PPARδ-responsive genes upon KD3010 treatment. KD3010, but not GW501516, protects cultured hepatocytes from starvation- and CCl_4-induced cell death. In fact, GW501516 increased ROS production and starvation-induced cell death in cultured hepatocytes. KD3010-mediated cytoprotection is PPARδ dependent, because the effect is lost in PPARδ-deficient hepatocytes. The mechanism likely involves expression of Cyp enzymes, which are stimulated by KD3010 and result in oxidation and detoxification of organic substances, whereas GW501516 did not alter expression of Cyp enzymes. In addition to the PPARδ-dependent cytoprotective effect, we also demonstrate the induction of CTGF by GW501516, which is a strong profibrotic cytokine. Combined, the cytoprotection and the absence of a profibrogenic cytokine confer protection against fibrosis and explain the differences between KD3010 and GW501516 observed in our study. Our study identifies hepatocytes as the main target cell population in the liver that mediates the beneficial effect of KD3010 in a PPARδ-dependent fashion.

Chronic liver disease results in hepatic fibrosis. The only current treatment paradigm for patients with hepatic fibrosis is treatment of the underlying liver disease (20). If the causative agent cannot be removed, there are currently no effective antifibrotic treatments for patients with chronic liver diseases (21). Experimental studies in rodents have revealed targets to prevent the progression of fibrosis. However, the efficacy of most treatments has not been tested in humans. Additionally, promising targets identified in rodents may result in undesirable side effects in humans. For example, inhibition of the profibrotic cytokine TGFβ-1 may favor cancer development, especially in liver cirrhosis, which is a premalignant state (2). On the other hand, PPARδ deficiency results in azoxymethane-induced regenerative liver cell hyperplasia, suggesting that PPARδ protects against enhanced cell proliferation in the liver (13). Insights into the mechanisms of the development of hepatic fibrosis provide an opportunity to develop therapeutic interventions for human clinical use. A PPARδ agonist may serve as a treatment option for liver fibrosis. The findings reported here should promote further clinical investigation into the potential use of a PPARδ agonist in treating patients with chronic liver diseases.

Materials and Methods

Mouse Models of Liver Fibrosis. Male 11-wk-old C57/B6 mice were treated with CCl_4 (2 μL/g body weight; 1:4 dilution with corn oil) or with corn oil as control (2 μL/g body weight) by i.p. injection every third day. Injections were repeated for a total of 12 times. Livers were harvested 3 d after the last injection. BDL or sham operation as control was performed as described previously (22), and livers were harvested 21 d later. All animal procedures were performed under the guidelines set by The University of California, San Diego Institutional Animal Care and Use Committee and are in accordance with those set by the National Institutes of Health.

Treatment Protocol. KD3010 (chemical name (S)-4-[cis-2,6-dimethyl-4-(4-trifluoromethoxy-phenyl)piperazine-1-sulfonyl]-indan-2-carboxylic acid tosylate) (Fig. S5) is a potent, orally active, and selective PPARδ agonist (Kalypsys Inc.). Phase I clinical trials have successfully been completed in healthy volunteers and demonstrated safety and tolerability without clinically relevant treatment- or dose-related trends in the laboratory, vital sign, ECG, or physical examination safety parameters (www.kalypsys.com). KD3010 has no appreciable interaction with human, rhesus, or murine PPARα and PPARγ receptors, as evidenced by EC_{50} values in excess of 7–10 μM. Cell-based reporter gene assays indicate that KD3010 (up to 10 μM) does not affect the function of mouse/human pregnane X receptor and human constitutive androstane receptor. For in vitro experiments we used concentrations of 1–5 μM. Mean plasma compound concentration of mice treated with CCl_4 and gavaged with KD3010 was 4 ± 0.8 μM (at time of harvesting). Mice were assigned randomly into groups at the beginning of the study. The study was conducted in a blinded fashion, and the researchers performing the in vivo

experiments (CCl_4 treatment and BDL; Figs. 1 and 2) remained blinded to the nature of the experimental drugs until all data were analyzed. Mice were treated daily with vehicle or KD3010 (10 mg/kg) by oral gavage. At times of CCl_4 injections, the compounds were administered 2 h after the last gavage was given. Similarly, a well-characterized PPARδ agonist GW501516 (2 mg/kg) or vehicle was administered to mice daily by gavage (6).

Liver Enzymes and Staining Procedures. Blood was taken at the time of harvesting. ALT in the plasma was measured by the Infinity kit (Thermo Fisher Scientific) according to the manufacturer's instructions. Formalin-fixed liver samples were embedded in paraffin and stained with H&E. Sirius Red staining [saturated picric acid containing 0.1% (wt/vol) Direct Red 80] was performed as described (22). The Sirius Red-positive area was measured at a final magnification of 40×. The entire median lobe of the liver was imaged, and 6–14 images per animal were taken and analyzed using National Institutes of Health Image J. The results are presented as percentage area positively stained for Sirius Red. Immunohistochemistry and immunofluorescence were performed using anti-PPARδ antibody (1:100; Santa Cruz), anti-desmin antibody (1:200; DAKO), and anti-F4/80 antibody (1:200; eBioscience) as described (22).

Hydroxyproline Measurement. Liver tissue was homogenized in ice-cold distilled water (900 μL) using a Power Gen homogenizer (Fisher). Subsequently, 125 μL of 50% (wt/vol) trichloroacetic acid was added, and the homogenates were incubated further on ice for 20 min. Precipitated pellets were hydrolyzed for 18 h at 110 °C in 6N HCL. After hydrolysis, the samples were filtered and neutralized with 10N NaOH, and the hydrolysates were oxidized with Chloramine-T (Sigma) for 25 min at room temperature. The reaction mixture then was incubated in Ehrlich's perchloric acid solution at 65 °C for 20 min and cooled to room temperature. Sample absorbance was measured at 560 nm in duplicate. Purified hydroxyproline (Sigma) was used to set a standard. Hydroxyproline content was expressed as nanogram of hydroxyproline per milligram liver.

Gene-Expression Analysis. Total RNA was extracted with TRIZOL (Invitrogen). RNA was digested with DNase using the DNA-free kit (Ambion). DNase-treated RNA was reverse transcribed using the High Capacity cDNA Reverse Transcription kit (ABI). Real-time quantitative PCR (qPCR) was performed for 40 cycles of 15 s at 95 °C and 60 s at 60 °C using an ABI 7000 sequence detection system. The relative abundance of the target genes was obtained by calculating against a standard curve and normalized to 18S or cyclophilin as internal control. Probes purchased from ABI or primers from the National Institutes of Health mouse qprimer depot were used with SYBR green (Bio-Rad). Microarrays were performed as described (6). Briefly, samples were labeled and hybridized to Affymetrix Mouse Genome 430 2.0 arrays (n = 3 in each group). Microarray data have been deposited in the Gene Expression Omnibus (accession code GSE32121). Microarray data analysis was performed as described (23). In brief, image data were converted into nonnormalized sample probe profiles using the BeadStudio software (Illumina) and analyzed on the VAMPIRE microarray analysis framework48. We constructed stable variance models for each of the two experimental conditions and identified differentially expressed probes using the unpaired VAMPIRE significance test with a two-sided, Bonferroni-corrected threshold (α_{Bonf}) of 0.05. The VAMPIRE statistical test is a Bayesian statistical method that computes a model-based estimate of noise at each level of gene expression. This estimate then was used to assess the statistical significance of the apparent differences in gene expression in the two experimental conditions.

Isolation and Culture of Hepatocytes, Kupffer Cells, and Hepatic Stellate Cells. Isolation of liver-cell fractions from normal liver using magnetic cell sorting (MACS) has been described (22). Kupffer cells and hepatic stellate cells were isolated from mice by two-step collagenase–pronase perfusion followed by three-layer discontinuous density gradient centrifugation with 8.2% (wt/vol) and 14.5% (wt/vol) Nycodenz (Accurate Chemical and Scientific Corporation) to obtain Kupffer-cell and hepatic stellate-cell fractions. Hepatic stellate cells were collected between the 0 and 8.2% (wt/vol) layer. The Kupffer-cell fraction was selected negatively by MACS using anti-LSEC Micro Beads (Miltenyi Biotech). Kupffer cells were cultured with DMSO or KD3010 (1 μM) for 1 d before stimulation by LPS (1 ng/mL for 4 h) or IL-4 (10 ng/mL for 24 h). Hepatic stellate cells were cultured with DMSO or KD3010 (5μM) for 3 d before harvesting. To induce starvation-associated cell death, hepatocytes were cultured in Waymouth's medium containing 10% (vol/vol) FCS for 3.5 h; Waymouth's medium then was changed to Krebs–Ringer buffer without glucose (KRB) in the presence of DMSO, KD3010 (5 μM), or GW501516 (100 nM). In some experiments, CCl_4 (2.5 mM) was added to hepatocytes after 12 h. Cell death was assessed by measuring ALT in the supernatant, by using a Cytotoxicity Detection Kit (Roche), or by staining with PI. Hepatocytes were isolated from wild-type or PPARδ-deficient mice (4) and were cultured in 96-well black-bottomed plates in KRB for 12 h in the presence of DMSO, KD3010 (5 μM), or GW501516 (100 nM). Cells were loaded with the redox-sensitive dye CM-H_2DCFDA (10 μM) diluted in KRB for 20 min at 37 °C. Cells then were rinsed twice with KRB and stimulated with CCl_4 (2.5 mM). CM-H_2DCFDA fluorescence was detected at excitation and emission wavelengths of 488 nm and 520 nm, respectively. ROS formation was measured in a time course of 23 min using a multiwell fluorescence scanner (Fluostar Optima; BMG Labtech). TBARS were measured by using OxiSelect TBARS Assay Kit (MDA Quantitation). For microarray analysis, RNA was extracted from hepatocytes cultured in Waymouth's medium containing 10% (vol/vol) FCS in the presence of DMSO, KD3010 (5 mM), or GW501516 (100 nM) for 12 h.

Statistical Analysis. Results are reported as mean ± SEM, unless otherwise stated. Comparisons among multiple groups were performed by one-way ANOVA with post hoc test (Tukey's Multiple Comparison Test). Mouse survival data were analyzed statistically by using the Log-rank (Mantel–Cox) test. Comparisons between two groups were performed by the Mann–Whitney u-statistic test. $P < 0.05$ was considered statistically significant. All statistical analyses were performed using GraphPad Prism.

ACKNOWLEDGMENTS. KD3010 was provided as a gift from Kalypsys, Inc. This study was supported in part by National Institutes of Health Grants K08 DK081830 and R01 AA020703 (to B.S.), R01 DK072237 (to D.A.B.), R01 DK057978 (to R.M.E.), and R24 DK090962 (to D.A.B. and R.M.E.). This study also was supported by University of California, San Diego Digestive Diseases Research Development Center Grant DK080506 (to B.S.) and by Award K12-HD000850 from the Eunice Kennedy Shriver National Institute of Child Health and Human Development (to E.Y.). R.M.E. was supported by the Helmsley Charitable Trust and by the Howard Hughes Medical Institute. R.M.E. is an investigator of the Howard Hughes Medical Institute and March of Dimes Chair in Molecular and Developmental Biology at the Salk Institute. E.Y. is a Fellow of the Pediatric Scientist Development Program.

1. Bataller R, Brenner DA (2005) Liver fibrosis. *J Clin Invest* 115:209–218.
2. Schnabl B, Scholten D, Brenner DA (2008) What is the potential role of antifibrotic agents for the treatment of liver disease? *Nat Clin Pract Gastroenterol Hepatol* 5: 496–497.
3. Barish GD, Narkar VA, Evans RM (2006) PPAR delta: A dagger in the heart of the metabolic syndrome. *J Clin Invest* 116:590–597.
4. Lee CH, et al. (2006) PPARdelta regulates glucose metabolism and insulin sensitivity. *Proc Natl Acad Sci USA* 103:3444–3449.
5. Oliver WR, Jr., et al. (2001) A selective peroxisome proliferator-activated receptor delta agonist promotes reverse cholesterol transport. *Proc Natl Acad Sci USA* 98: 5306–5311.
6. Narkar VA, et al. (2008) AMPK and PPARdelta agonists are exercise mimetics. *Cell* 134: 405–415.
7. Odegaard JI, et al. (2008) Alternative M2 activation of Kupffer cells by PPARdelta ameliorates obesity-induced insulin resistance. *Cell Metab* 7:496–507.
8. Magness ST, Bataller R, Yang L, Brenner DA (2004) A dual reporter gene transgenic mouse demonstrates heterogeneity in hepatic fibrogenic cell populations. *Hepatology* 40:1151–1159.
9. Olefsky JM, Glass CK (2010) Macrophages, inflammation, and insulin resistance. *Annu Rev Physiol* 72:219–246.
10. Kang K, et al. (2008) Adipocyte-derived Th2 cytokines and myeloid PPARdelta regulate macrophage polarization and insulin sensitivity. *Cell Metab* 7:485–495.
11. Gressner OA, Gressner AM (2008) Connective tissue growth factor: A fibrogenic master switch in fibrotic liver diseases. *Liver Int* 28:1065–1079.
12. Kodama T, et al. (2011) Increases in p53 expression induce CTGF synthesis by mouse and human hepatocytes and result in liver fibrosis in mice. *J Clin Invest* 121:3343–3356.
13. Shan W, et al. (2008) Peroxisome proliferator-activated receptor-beta/delta protects against chemically induced liver toxicity in mice. *Hepatology* 47:225–235.
14. Shan W, et al. (2008) Ligand activation of peroxisome proliferator-activated receptor beta/delta (PPARbeta/delta) attenuates carbon tetrachloride hepatotoxicity by downregulating proinflammatory gene expression. *Toxicol Sci* 105:418–428.
15. Hellemans K, et al. (2003) Peroxisome proliferator-activated receptor-beta signaling contributes to enhanced proliferation of hepatic stellate cells. *Gastroenterology* 124: 184–201.
16. Knight B, Yeap BB, Yeoh GC, Olynyk JK (2005) Inhibition of adult liver progenitor (oval) cell growth and viability by an agonist of the peroxisome proliferator activated receptor (PPAR) family member gamma, but not alpha or delta. *Carcinogenesis* 26: 1782–1792.
17. Downes M, et al. (2003) A chemical, genetic, and structural analysis of the nuclear bile acid receptor FXR. *Mol Cell* 11:1079–1092.

18. Marathe C, et al. (2009) Preserved glucose tolerance in high-fat-fed C57BL/6 mice transplanted with PPARgamma-/-, PPARdelta-/-, PPARgammadelta-/-, or LXRalphabeta-/- bone marrow. *J Lipid Res* 50:214–224.
19. Bouhlel MA, et al. (2009) Unlike PPARgamma, PPARalpha or PPARbeta/delta activation does not promote human monocyte differentiation toward alternative macrophages. *Biochem Biophys Res Commun* 386:459–462.
20. Poynard T, et al. (2002) Impact of pegylated interferon alfa-2b and ribavirin on liver fibrosis in patients with chronic hepatitis C. *Gastroenterology* 122:1303–1313.
21. Di Bisceglie AM, et al.; HALT-C Trial Investigators (2008) Prolonged therapy of advanced chronic hepatitis C with low-dose peginterferon. *N Engl J Med* 359: 2429–2441.
22. Taura K, et al. (2008) Hepatic stellate cells secrete angiopoietin 1 that induces angiogenesis in liver fibrosis. *Gastroenterology* 135:1729–1738.
23. Pei L, et al. (2011) Thyroid hormone receptor repression is linked to type I pneumocyte-associated respiratory distress syndrome. *Nat Med* 17:1466–1472.